State-of-the-art density matrix renormalization group and coupled cluster theory studies of the nitrogen binding curve

Garnet Kin-Lic ChanMihály Kállay and Jürgen Gauss

Citation: **121**, (2004); doi: 10.1063/1.1783212
View online: http://dx.doi.org/10.1063/1.1783212
View Table of Contents: http://aip.scitation.org/toc/jcp/121/13
Published by the American Institute of Physics

RIGHTSLINK

HTML ABSTRACT + LINKS

ARTICLES

State-of-the-art density matrix renormalization group and coupled cluster theory studies of the nitrogen binding curve

Garnet Kin-Lic Chan[a)]
Department of Chemistry, University of Cambridge, Cambridge CB2 1EW, United Kingdom

Mihály Kállay and Jürgen Gauss
Institut für Physikalische Chemie, Universität Mainz, D-55099 Mainz, Germany

(Received 27 May 2004; accepted 24 June 2004)

We study the nitrogen binding curve with the density matrix renormalization group (DMRG) and single-reference and multireference coupled cluster (CC) theory. Our DMRG calculations use up to 4000 states and our single-reference CC calculations include up to full connected hextuple excitations. Using the DMRG, we compute an all-electron benchmark nitrogen binding curve, at the polarized, valence double-zeta level (28 basis functions), with an estimated accuracy of 0.03 mE_h. We also assess the performance of more approximate DMRG and CC theories across the nitrogen curve. We provide an analysis of the relative strengths and merits of the DMRG and CC theory under different correlation conditions. © *2004 American Institute of Physics.*
[DOI: 10.1063/1.1783212]

I. INTRODUCTION

High-accuracy numerical studies of the Schrödinger equation allow us to assess approximate methods and the contribution of higher-level corrections to molecular properties. These studies are of particular interest in challenging systems, which possess complicated electronic structure.

In this work, we examine the well-known problem of the nitrogen binding curve. As the nitrogen triple bond is stretched, the electronic structure changes from single-reference to highly multireference, and consequently a balanced description across the potential energy curve has traditionally been difficult to achieve.[1,2,3,4–6]

Here, we use the density matrix renormalization group (DMRG) and high-level coupled cluster (CC) theories to compute a benchmark, all-electron, nitrogen binding curve within the Dunning cc-pVDZ basis.[7] These calculations thus go beyond previous full configuration interaction (FCI) studies, which used the frozen-core $(10\,e)$ approximation.[1,6] All-electron FCI calculations [which retain all elements of the configuration interaction (CI) vector] for this system remain currently out of reach (the D_{2h} space contains roughly 1.8×10^{11} determinants). While the DMRG and CC theories should be seen as providing a hierarchy of approximations to the FCI result, our calculations have been carried out to a very high level ($M=4000$ for DMRG, and up to hextuple excitations for CC theory), yielding near-FCI quality numerical results. Our best DMRG calculations yield an estimated residual error across the nitrogen binding curve of better than $0.03mE_h$, and, in the equilibrium region, even higher accuracy is achieved by our best CC results.

In addition to the benchmark calculations, we examine the behavior of both approximate DMRG and CC (single reference and multireference) theories for the nitrogen dissociation problem. A particular question we seek to answer is the relative suitability of the DMRG and CC theories in bond-breaking situations. This study leads us to conclude with an analysis of the relative merits of the two approaches under different correlation conditions.

II. METHODOLOGY

A. DMRG

The DMRG is a method to systematically approximate the solution of the Schrödinger equation. It has been widely applied to study strongly-correlated quantum lattices[8,9] and has more recently been developed as a quantum chemical method.[10–15] As a detailed description of our algorithm and implementation may be found in Refs. 12 and 14 we shall concentrate on the conceptual aspects of the method.

We first partition orbitals into two groups: a left and right block with l and r orbitals. In general, the Fock space of each block F_l, F_r is spanned by a set of many-particle functions $\{\chi_l\}$, $\{\chi_r\}$, and thus the exact wave function of the system may be written as

$$\Psi=\sum_{\lambda\mu} d_{\lambda\mu}|\chi_l^\lambda\rangle|\chi_r^\mu\rangle=\sum_\lambda c_\lambda|\chi_l^\lambda\rangle|\phi_r^\lambda\rangle, \tag{1}$$

where $\phi_r^\lambda=\Sigma_\mu d_{\lambda\mu}\chi_r^\mu$, and the sum in Eq. (1) is subject to necessary constraints, e.g., if the system has a definite number of particles N, then the number of particles in χ_l and ϕ_r must add up to N.

In the DMRG, we seek the best approximation of rank $4M$ to Ψ Ref. 16, and thus the DMRG Ansatz is

[a)]Present address: Department of Chemistry and Chemical Biology, Cornell University, Ithaca, NY 14853-1301.

 © 2004 American Institute of Physics

RIGHTSLINK

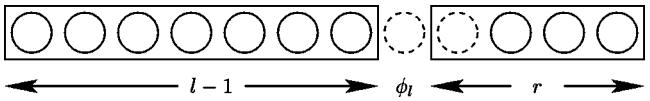

FIG. 1. A typical block configuration, with $l-1$ orbitals (circles) in the left block, r orbitals in the right block, and a single orbital (dashed circle) ϕ_l (4 states) to be added to the left block. For simplicity, the orbital that is added to the right block (dashed circle) is considered as part of the right block here.

$$\Psi = \sum_{\lambda}^{4M} c_{\lambda} |\psi_l^{\lambda}\rangle |\psi_r^{\lambda}\rangle, \tag{2}$$

where $\psi_l^{\lambda}, \psi_r^{\lambda}$ are now optimal many-particle functions in the Fock spaces of the left and right blocks. The Ansatz (2) amounts to a singular value decomposition of Ψ where $\psi_l^{\lambda}, \psi_r^{\lambda}$ are the singular vectors and c_{λ} are the weights. Equivalently, in a procedure from which the method derives its name, we can compute ψ_l^{λ} as the eigenvectors of the reduced density matrix $\Gamma = \mathrm{Tr}_{\{r\}} |\Psi\rangle\langle\Psi|$, where we have traced over the states in the right-hand block. Because the functions $\psi_l^{\lambda}, \psi_r^{\lambda}$ are optimal many-particle functions, and not simply determinants, it is possible for Eq. (2) to provide a compact representation of Ψ for relatively small values of M.

The objective of the DMRG algorithm is then to determine the optimal functions $\psi_l^{\lambda}, \psi_r^{\lambda}$. To facilitate this, the DMRG assumes an additional nested structure—typical of a renormalization group theory—that relates the functions in successively larger blocks,

$$\{\psi_l^{\lambda}\} \in \{\phi_l\} \otimes \{\psi_{l-1}^{\lambda}\}, \tag{3}$$

that is, the optimal functions for the block l are contained within the product Fock space of the smaller block $l-1$ and orbital ϕ_l (see Fig. 1). At each length of block l, the optimal M functions ψ_l^{λ} are determined by solving the Schrödinger equation with the best current representations $\{\psi_r^{\lambda}\}$ and $\{\psi_{l-1}^{\lambda}\}$ in the tensor product space of $O(16M^2)$ functions, and constructing the reduced density matrix of the left-hand block to determine the $O(4M)$ eigenvectors ψ_l^{λ} (of which we retain M). Thus DMRG calculations are performed in an iterative set of sweeps, where in each sweep, one block is increased in size at the expense of the other, while the representations of the spaces ($\{\psi_l^{\lambda}\}$ or $\{\psi_r^{\lambda}\}$ depending on the direction of the sweep) are improved.

As we sweep through the orbitals to construct our spaces in Eq. (3), we need to specify an order in which the orbitals are traversed. In one-dimensional systems, a natural ordering consistent with the hierarchical space structure (3) exists and in such systems, the DMRG is particularly powerful. However, we do not have this natural ordering in most molecules, and in practice, we commonly order by grouping orbitals together to minimize long-range correlations (and thus the number of interactions between the left and right blocks), or simply energy order by orbital eigenvalue.[12,17,18]

The DMRG wave function exists within a product Ansatz, and thus with a physical ordering, the DMRG is a size-consistent theory. Consider a system with two noninteracting widely-separated fragments A,B and with orbitals $\{a\}$ on A and $\{b\}$ on B. Now order the orbitals, $\{a\}\{b\}$, so that the orbitals on A and B form two disjoint sets. If we now place the dividing line between the left and right blocks between $\{a\}$ and $\{b\}$, then the DMRG Ψ is immediately in the separable size-consistent product form $\Psi = \psi_A \psi_B$,[19] where ψ_A, ψ_B are the corresponding rank M DMRG wave functions for A, B.

B. Coupled cluster theory

Excellent treatments of CC theory may be found in the literature[20,21] and we provide only a brief review. In CC theory, the wave function is expressed by the exponential Ansatz

$$\Psi = e^T |0\rangle, \tag{4}$$

where $|0\rangle$ is the reference, usually a Hartree–Fock determinant, and T is an excitation operator,

$$T = \sum_n T_n, \tag{5}$$

e.g.,

$$T_1 = \sum_{ia} t_i^a a_a^{\dagger} a_i, \tag{6}$$

$$T_2 = \frac{1}{4} \sum_{ijab} t_{ij}^{ab} a_a^{\dagger} a_b^{\dagger} a_i a_j, \tag{7}$$

where i,j denote orbitals occupied in $|0\rangle$ and a,b denote the corresponding unoccupied virtuals. The important feature of the CC Ansatz is the separation of correlation into connected and disconnected components; for example, double excitations from $ij \rightarrow ab$ are expressed as the sum of a (disconnected) product of single excitations due to $(1/2)T_1^2$ and a connected contribution T_2. A truncated T operator yields a good representation of the wave function when the neglected connected components are small. In addition, truncated CC Ansätze are size consistent since $e^{T_{AB}} = e^{T_A + T_B} = e^{T_A} e^{T_B}$, if T_A and T_B act only on A and B, respectively, since the CC equations are fully connected.

The CC equations to determine the T amplitudes are nonlinear equations with a number of terms that grow factorially with excitation order n. This has led to several different computational strategies to handle the complexity of high order CC theory.[22–26] In this work, we use a string-based algorithm[23,27] to evaluate excitations of arbitrary order.

C. Multireference coupled cluster and configuration interaction

In our study of approximate methods (Sec. III C) we present calculations using the multireference configuration interaction (MRCI) and multireference coupled cluster (MRCC) theories. These were developed to describe the kind of correlation problems we encounter in the current work, i.e., bond breaking, where the Hartree–Fock reference is a poor representation. In these methods, the Hartree–Fock reference is replaced by a set of reference determinants, often chosen to be a complete active space, and usually single and double excitations out of the reference determinants are con-

RIGHTSLINK

TABLE I. Frozen-core correlation energies (relative to the RHF reference) for DMRG, CC, FCI, and RHF total energies. All results in E_h. *Italics* denote unconverged digits.

	$2.118a_0$	$2.4a_0$	$2.7a_0$	$3.0a_0$	$3.6a_0$	$4.2a_0$
RHF	−108.949 378	−108.866 811	−108.737 400	−108.606 226	−108.384 757	−108.222 899
FCI	−0.328 961	−0.371 586	−0.422 905	−0.479 983	−0.610 149	−0.744 051
DMRG: 1000	−0.3286	−0.3712	−0.4225	−0.4794	−0.6095	−0.7434
DMRG: 2000	−0.328 90	−0.371 51	−0.422 83	−0.479 86	−0.610 01	[a]
DMRG: 4000	−0.328 95*1*	−0.371 57*5*	−0.422 89*3*	−0.479 96*3*	−0.610 129	[a]
CCSD	−0.314 493	−0.350 105	−0.391 098	−0.434 795	−0.537 926	−0.703 353
CCSD(T)	−0.327 095	−0.368 499	−0.417 723	−0.472 283	−0.616 179	−0.909 065
CCSDT	−0.327 122	−0.367 955	−0.416 071	−0.469 673	−0.626 097	−0.857 182
CCSDTQ	−0.328 732	−0.371 003[b]	−0.421 548[b]	−0.477 57[b]	−0.6096[b]	[c]
CCSDTQP	−0.328 940	[a]	[a]	[a]	[c]	[c]
CCSDTQPH	−0.328 959	[a]	[a]	[a]	[c]	[c]
MRCI	−0.322 307	−0.364 763	−0.415 928	−0.472 865	−0.602 969	−0.737 138
MRCC	−0.327 446	−0.370 058	−0.421 287	−0.478 194	−0.607 962	−0.741 805
UHF-CCSD	−0.314 493	−0.349 551	−0.390 925	−0.443 632	−0.588 181	−0.734 422
UHF-CCSD(T)	−0.327 095	−0.365 210	−0.409 908	−0.459 480	−0.595 061	−0.737 125
UHF-CCSDT	−0.327 122	−0.367 663	−0.415 941	−0.469 972	−0.602 663	−0.740 928
UHF-CCSDTQ	−0.328 732	−0.370 936	−0.421 467	−0.476 969	−0.605 808	−0.742 138
UHF-CCSDTQP	−0.328 940	−0.371 445	−0.422 557	−0.479 164	−0.607 796	−0.742 907
UHF-CCSDTQPH	−0.328 959	−0.371 514	−0.422 771	−0.479 781	−0.609 405	−0.743 224

[a]Not computed due to computer time constraints.
[b]Taken from Ref. 1.
[c]Not computed due to convergence difficulties.

sidered. In a MRCI calculation the Hamiltonian is simply diagonalized in this space. The main formal disadvantage of MRCI is the lack of size consistency.

Among the several multireference generalizations of CC theory, we employ the state-selective MRCC Ansatz proposed originally by Oliphant and Adamowicz.[28] In this approach a formal Fermi vacuum is chosen from the reference space and excitations out of the other reference functions are regarded as higher excitations from this determinant. The appealing feature of this method is that it retains the simplicity and the size-extensive nature of the single-reference CC formalism. More detailed descriptions of MRCI and MRCC theories may be found in Ref. 29.

III. THE NITROGEN BINDING CURVE

A. Methodology

Calculations on the nitrogen molecule were carried out using the Dunning *cc-p*VDZ basis[7] with spherical *d* functions (28 basis functions in total). Six geometries were studied: 2.118 (r_e), 2.4, 2.7, 3.0, 3.6, $4.2a_0$. Frozen-core calculations employed both canonical restricted Hartree–Fock (RHF) and unrestricted Hartree–Fock (UHF) orbitals (energies given in Tables I and III), freezing the $1\sigma_g$, $1\sigma_u^*$, or nitrogen 1s orbitals. All-electron calculations used canonical UHF orbitals. Molecular orbital calculations were performed and integrals were computed using MOLPRO.[30]

FCI calculations in D_{2h} symmetry were computed at the frozen-core level using the program of Kállay *et al.*[23]

DMRG calculations used the BLOCK program.[14] Two warm-up sweeps at $M=600$, 800 were carried out, followed by sweeps at $M=1000$, 2000, 4000. The number of sweeps at each M value ranged from 6–17 sweeps at the $M=1000$ level, to 4–6 sweeps at the $M=4000$ level; all sweep energies are reported to the number of converged digits. Orbitals were ordered to minimize long-range interactions as measured by the one-electron integrals (orderings available as supplementary material). Since the one-electron integrals vanish between orbitals of different symmetry, these reorderings group orbitals of the same symmetry together. For technical reasons[31] the DMRG calculations were carried out using only C_s symmetry.

Single-reference CC calculations including up to hextuple excitations were carried out using the program of Kállay *et al.*[23] CCSD (T) energies were obtained using ACES II.[32] At the all-electron level we neglected hextuple excitations out of the nitrogen 1*s* orbitals: this frozen-core approximation is denoted H-fc. We estimate the error with respect to full CCSDTQPH since this approximation is in the range of 0.1–0.2 μE_h. All CC calculations used the full symmetry group of the orbitals (C_{2v} or D_{2h}) and were converged to the μE_h level.

MRCISD and MRCCSD calculations were obtained using the program of Kállay *et al.*[27] A complete active space (CAS) containing the nitrogen $3\sigma_g^+$, $1\pi_u$, $1\pi_g$, $3\sigma_u^+$ orbitals was used. The (6, 6) CAS wave function was used as the reference space in the subsequent MRCCSD calculations. Multiconfigurational self-consistent-field calculations were performed and integrals were obtained using the COLUMBUS[33] suite of programs.

B. Frozen-core calibration calculations

Before presenting our all-electron results, we first present frozen-core calculations, which allow us to calibrate

RIGHTSLINK

TABLE II. Errors in frozen-core correlation energies, relative to FCI (all energies in mE_h). NPE = abs(maximum error − minimum error). *Italics* denote unconverged digits.

	$2.118a_0$	$2.4a_0$	$2.7a_0$	$3.0a_0$	$3.6a_0$	$4.2a_0$	NPE
DMRG: 1000	0.3	0.4	0.4	0.6	0.7	0.6	0.4
DMRG: 2000	0.06	0.07	0.08	0.12	0.14	[a]	0.08
DMRG: 4000	0.01*0*	0.01*1*	0.01*2*	0.01*9*	0.02*0*	[a]	0.01*0*
CCSD	14.469	21.481	31.807	45.188	72.223	40.698	57.754
CCSD(T)	1.866	3.087	5.182	7.700	−6.030	−165.014	172.714
CCSDT	1.839	3.631	6.834	10.310	−15.948	−113.131	123.441
CCSDTQ	0.229	0.583[b]	1.357[b]	2.41[b]	0.5[b]	[c]	2.181
CCSDTQP	0.021	[a]	[a]	[a]	[c]	[c]	[c]
CCSDTQPH	0.002	[a]	[a]	[a]	[c]	[c]	[c]
MRCI	6.654	6.823	6.977	7.118	7.180	6.913	0.464
MRCC	1.515	1.529	1.618	1.789	2.187	2.247	0.732
UHF-CCSD	14.468	22.035	31.981	36.351	21.968	9.630	26.721
UHF-CCSD(T)	1.866	6.376	12.997	20.503	15.088	6.926	18.637
UHF-CCSDT	1.839	3.923	6.964	10.011	7.486	3.123	8.172
UHF-CCSDTQ	0.229	0.651	1.438	3.014	4.341	1.913	4.112
UHF-CCSDTQP	0.021	0.141	0.348	0.819	2.353	1.144	2.332
UHF-CCSDTQPH	0.002	0.073	0.134	0.202	0.744	0.827	0.825

[a]Not computed due to computer time constraints.
[b]Taken from Ref. 1.
[c]Not computed due to convergence difficulties.

our DMRG and CC methods against FCI. Our computed energies and errors from FCI are presented in Tables I, II, and Fig. 2.

We remark first on the convergence of the DMRG sweeps for fixed M. The presented sweep energies are given to fewer than six digits at the $M=1000$, 2000 level. While successive sweeps at fixed M typically converge smoothly (see Fig. 3), the rate of convergence slows when the remaining sweep error is comparable to the intrinsic error associated with truncation to M states. This slowdown results from the simple self-consistent sweep procedure employed in our DMRG algorithm. Consequently, given our computing resource constraints, it is wasteful to converge small M calculations to very high accuracy. Convergence is also slower at stretched geometries, but we typically require no more than two to three times the number of sweeps to achieve the same level of convergence as at r_e. Acceleration schemes such as direct inversion in the iterative subspace (DIIS)[34] may be used to improve the self-consistent DMRG sweep procedure in the future.

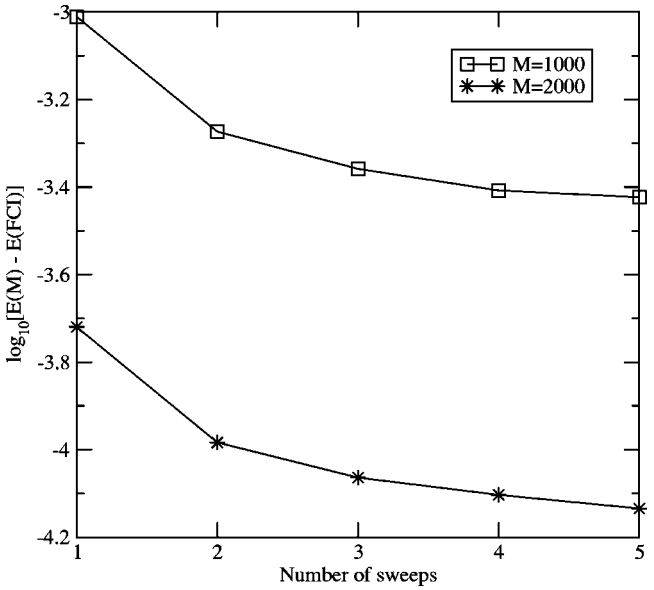

FIG. 2. Frozen-core energy errors for the nitrogen curve, measured relative to FCI energies.

The DMRG energies at all M values display an error across the potential energy curve that varies only within a factor of 2. The most accurate calculations at $M=4000$ had a maximum error of $20\mu E_h$, and a nonparallelity error (the absolute difference between the maximum and minimum errors) of only $10\mu E_h$. This is encouraging given the multireference nature of the problem, and demonstrates the insensitivity of the DMRG to the quality of the underlying RHF reference, which is very poor at stretched geometries.

The current results improve over our previous calculations in Ref. 12, which displayed an artificial increase in error in the intermediate bonding regime. This is due to our use of the improved sweep initialization procedure described in Ref. 14, which prevents the loss of quantum numbers during the early warm-up sweeps.

We now turn to our CC calculations. The earlier study of Krogh and Olsen[1] already presented frozen-core FCI and CC calculations including up to quadruple excitations at a number of points along the nitrogen curve. We have, when possible, recomputed more fully converged FCI and CC energies, and extended the calculations of Krogh and Olsen to highly stretched geometries. We have been unable to obtain CC results using the RHF reference at the higher excitation levels at $4.2a_0$. This is due, in part, to the poor convergence behavior of the CC equations. For example, at $4.2a_0$, the CCSDT equations required over 500 iterations to converge,

RIGHTSLINK

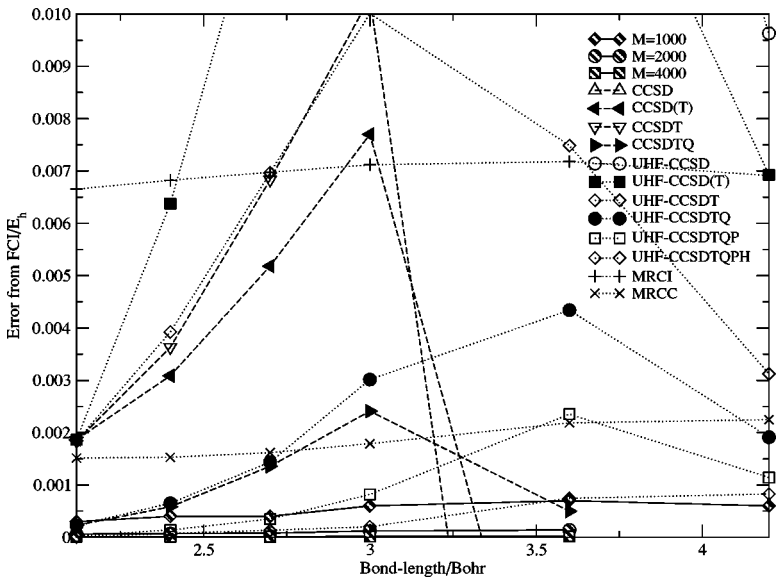

FIG. 3. Convergence of the DMRG energy/E_h (at *fixed* M) as a function of the number of sweeps.

and we could not converge the CCSDTQ energy even after many hundreds of iterations. This is a reflection of the breakdown of the restricted CC description at long bond lengths. In agreement with this breakdown, the error in the CC energies increases by an order of magnitude as the bond is stretched. Furthermore, the CCSDT energy actually lies significantly below the variational limit (Table II) at longer bond lengths. This pathological behavior contrasts with the behavior at equilibrium, where the convergence of the CC hierarchy is exponential and the CCSDTQPH energy is in error by only $2\mu E_h$.

Although the unrestricted CC energies were obtained with an unrestricted frozen core, and are thus not strictly comparable with the other results, the effect of the change of core is quite small. To estimate this effect, we performed a frozen-core unrestricted FCI calculation at $2.4a_0$, yielding a correlation energy (relative to the RHF reference) of $-0.371\,520E_h$, $66\mu E_h$ above the restricted FCI result. This difference is small enough to allow us to comment on the change when going from the restricted to the unrestricted CC theory. In general, we observe a crossover between the accuracies of restricted CC and unrestricted CC energies at $3.0a_0$ (roughly $1.5r_e$). However, although the unrestricted CC theories avoid a variational catastrophe at longer bond lengths, the convergence of the unrestricted CC hierarchy to the FCI result is still very slow. Thus, even with full hextuple excitations, the error at $4.2a_0$ is $0.827\mathrm{M}E_h$, 400 times larger than at r_e.

Finally, we comment briefly on our MRCI and MRCC results. Both theories produce well-behaved dissociation curves. It should be noted that although the absolute errors of the MRCI energies are far greater than the MRCC energies, the nonparallelity errors (NPEs) are within a factor of 2. This is particularly significant given the greatly increased cost when going from MRCI to MRCC theory.

C. All-electron calculations

In Table III and Fig. 4 we present new all-electron calculations using the DMRG, CC, MRCI, and MRCC meth-

TABLE III. All-electron nitrogen correlation energies using DMRG and CC theories and UHF total energies. All results in hartrees. Core correlation energy = DMRG($M = 4000$) − FCI(frozen core). *Italics* denote unconverged digits.

	$2.118a_0$	$2.4a_0$	$2.7a_0$	$3.0a_0$	$3.6a_0$	$4.2a_0$
UHF	−108.949 378	−108.891 623	−108.833 687	−108.790 272	−108.767 549	−108.775 057
DMRG: 1000	−0.3325	−0.3498	−0.3294	−0.2985	−0.2300	−0.1946
DMRG: 2000	−0.332 71	−0.350 18	−0.329 78	−0.298 98	−0.230 39	−0.194 95
DMRG: 4000	−0.332 779	−0.350 263	−0.329 885	−0.299 103	−0.230 503	−0.195 033
CCSD	−0.318 248	−0.328 171	−0.297 804	−0.262 607	−0.208 336	−0.185 187
CCSD(T)	−0.330 927	−0.343 952	−0.316 958	−0.278 592	−0.215 287	−0.187 928
CCSDT	−0.330 945	−0.346 407	−0.323 016	−0.289 165	−0.222 969	−0.191 795
CCSDTQ	−0.332 565	−0.349 698	−0.328 577	−0.296 225	−0.226 187	−0.193 067
CCSDTQP	−0.332 774	−0.350 209	−0.329 676	−0.298 450	−0.228 250	−0.193 901
CCSDTQPH-fc	−0.332 794	−0.350 278	−0.329 890	−0.299 067	−0.229 859	−0.194 217
MRCISD	−0.325 978	−0.343 302	−0.322 786	−0.291 872	−0.223 210	−0.188 013
MRCCSD	−0.331 268	−0.348 739	−0.328 282	−0.297 336	−0.228 336	−0.192 808
Core	−0.003 82	−0.003 49	−0.003 27	−0.003 17	−0.003 15	−0.003 14

RIGHTSLINK

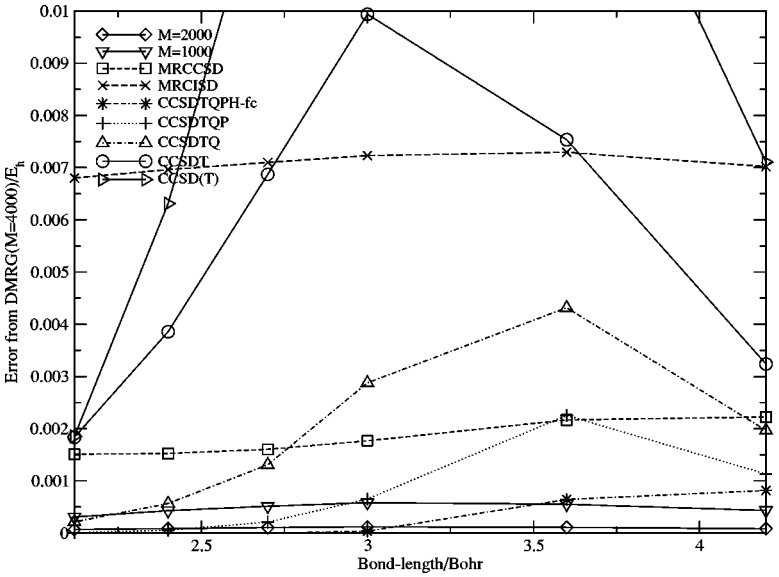

FIG. 4. All-electron energy errors for the nitrogen curve, measured relative to DMRG ($M=4000$) energies.

ods. We expect balanced results over the entire binding curve to be provided by our highest level DMRG ($M=4000$) calculation. While we cannot give a definitive estimate of the error of our calculations in the absence of exact results, we can refer to our previous experience in the frozen-core calculations. At the frozen-core level at r_e, the DMRG ($M=4000$) number is accurate to $9.5\mu E_h$, while the CCSDTQPH energy is essentially exact. We observe a comparable energy difference of $15\mu E_h$ between the all-electron DMRG ($M=4000$) and CCSDTQPH-fc numbers, indicating that errors in the correlation energies should be roughly transferable. From our frozen-core calculations, we also expect a slowly varying error in the DMRG energy across the potential energy curve; allowing the same factor of 2 variation in the error, we estimate that our DMRG ($M=4000$) correlation energies are accurate to better than $30\mu E_h$ across the nitrogen curve.

We note that we observe similar convergence (with M) of the DMRG algorithm both in the all-electron calculations, which used *localized* unrestricted orbitals, and the frozen-core calculations which used *delocalized* restricted orbitals. Although a localized description might appear to be beneficial for the DMRG, in practice the advantages are reduced in systems which are not one dimensional, as is the case here.

The CC correlation energies lie below the DMRG ($M=4000$) energies at the geometries near equilibrium, with the crossover between the CCSDTQPH-fc and DMRG ($M=4000$) energies occurring at roughly $2.7a_0$. However, as expected, the error in the single-reference CC calculations grows as the bond is stretched, which results from the poor quality of the Hartree–Fock reference at stretched geometries. Thus whereas the CCSDTQPH-fc energy is expected to be accurate to a few μE_h at r_e, at $4.2a_0$ (roughly $2r_e$), the energy lies about $0.84\mathrm{M}E_h$ above the best DMRG result. Since the CCSDTQPH-fc wave function contains the full active space, this NPE is attributable to the different treatment of dynamic correlation across the binding curve. Lower level CC methods display a characteristic maximum in the error near $3.6a_0$. Furthermore, the commonly used CCSD (T) approximation yields substantially different energies from CCSDT theory at stretched geometries.

The MRCISD and MRCCSD curves display large absolute errors (due to the incomplete treatment of dynamic correlation) but the error curves are quite flat, and the NPEs are relatively small in comparison to the error in the total energy. As the NPEs for both MR schemes are very similar, it appears that the size-consistency problem of MRCI is an unimportant issue for the calculation of the potential energy curve of N2.

Our all-electron calculations allow us to estimate the core-correlation energy. As expected, the core-correlation energy [estimated from the DMRG ($M=4000$) energies] smoothly decreases as the bond is stretched, decreasing from $3.8\mathrm{M}E_h$ (r_e) to $3.1\mathrm{M}E_h$ ($4.2a_0$).

Finally, a few remarks concerning the cost of these calculations. The time taken per DMRG sweep for the all-electron calculations was roughly 0.56/1.6/8.5 h at the $M=1000/2000/4000$ levels using 64 1.05 GHz Sun UltraSparc IIICu processors. It should be noted that the all-electron DMRG calculations are *not* much more expensive than the frozen-core calculations which take 0.39 1.1 or 5.0 h, respectively, at the same M levels; the theoretical quartic scaling yields a cost ratio of 1.4 between all-electron and frozen core calculations. The CCSDTQPH-fc calculations took roughly 1 day per CC iteration on a 2.4 GHz Pentium IV workstation, with a total number of iterations ranging from 7 at r_e to 100 at $4.2a_0$.

IV. EXCITATIONS IN DMRG AND CC THEORY

Although both the CC and DMRG hierarchies represent correlated wave functions in compact, and hence efficient forms, the two theories encompass significantly different models of correlations, with different strengths. As is well known, CC methods typically provide an efficient representation of correlated wave functions near the equilibrium region. While the CCSDTQPH-fc wave function is still *less* compact than the DMRG ($M=4000$) wave function, in that

RIGHTSLINK

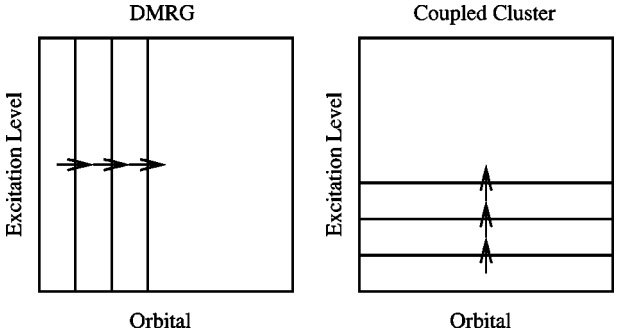

FIG. 5. Excitations in DMRG and CC theory. In the DMRG, all levels of excitation to and from a given orbital are considered before truncation. In CC theory, excitations are truncated based on their order relative to the reference.

there are far more than 4000 CC amplitudes [or even 300 000, the typical size of the full $O(16M^2)$ tensor product DMRG space at the $M=4000$ level], we note that the high overhead associated with the RG methodology means that in practice it is typically more costly to perform a DMRG calculation of comparable accuracy to a high-level CC calculation at r_e. While the CC hierarchy makes use of a connected or disconnected representation of excitations, the DMRG makes no such distinction.

The weakness of the CC hierarchy lies in the favored status given to the reference system. Thus high-level excitations, as measured from the reference, are truncated first. This order of truncation is illustrated schematically in Fig. 5. In contrast, the DMRG provides a radically different scheme of truncation, where excitations are truncated to and from *each* given orbital, as illustrated in Fig. 5. Thus the DMRG treats all orbitals on an equal footing and is a true multireference theory. This accounts naturally for the much improved performance of the DMRG as compared to CC theory in multireference scenarios.

V. CONCLUSIONS

In this work we have carried out benchmark frozen-core and all-electron studies of the nitrogen molecule binding curve, using state-of-the-art DMRG and CC methods. Using the DMRG, we have been able to provide near-full-CI-quality (within $30\mu E_h$) solutions of the Schrödinger equation.

Our investigations demonstrate that the CC theories provide very good representations of correlation near equilibrium, but even with fully connected hextuple excitations, this description rapidly worsens at more stretched geometries. In contrast, the DMRG provides a much better balanced description across the full potential surface, although near the equilibrium geometry, this representation can be less efficient than that provided by CC theory.

ACKNOWLEDGMENTS

This work was supported by Christ's College, Cambridge, and the Fonds der Chemischen Industrie.

[1] J. W. Krogh and J. Olsen, Chem. Phys. Lett. **344**, 578 (2001).
[2] W. D. Laidig, P. Saxe, and R. J. Bartlett, J. Chem. Phys. **86**, 887 (1987).
[3] S. R. Gwaltney, E. F. C. Byrd, T. V. Voorhis, and M. Head-Gordon, Chem. Phys. Lett. **353**, 359 (2002).
[4] X. Li and J. Paldus, Chem. Phys. Lett. **286**, 145 (1998).
[5] S. A. Kucharski, J. D. Watts, and R. J. Bartlett, Chem. Phys. Lett. **302**, 295 (1999).
[6] H. Larsen, J. Olsen, P. Jørgensen, and O. Christiansen, J. Chem. Phys. **113**, 6677 (2000).
[7] T. H. Dunning, Jr., J. Chem. Phys. **53**, 2823 (1989).
[8] S. R. White, Phys. Rev. Lett. **69**, 2863 (1992).
[9] S. R. White, Phys. Rev. B **48**, 10345 (1993).
[10] S. R. White and R. L. Martin, J. Chem. Phys. **110**, 4127 (1999).
[11] A. O. Mitrushenkov, G. Fano, F. Ortolani, R. Linguerri, and P. Palmieri, J. Chem. Phys. **115**, 6815 (2001).
[12] G. K.-L. Chan and M. Head-Gordon, J. Chem. Phys. **116**, 4462 (2002).
[13] G. K.-L. Chan and M. Head-Gordon, J. Chem. Phys. **118**, 8551 (2003).
[14] G. K.-L. Chan, J. Chem. Phys. **120**, 3172 (2004).
[15] Ö. Legeza, J. Roder, and B. A. Hess, Mol. Phys. **101**, 2019 (2003).
[16] The factor of 4 arises from the contribution of the Fock space of the orbital that is being added to the growing block.
[17] A. O. Mitrushenkov, R. Linguerri, P. Palmieri, and G. Fano, J. Chem. Phys. **119**, 4148 (2003).
[18] Ö. Legeza and J. Sólyom, Phys. Rev. B **68**, 195116 (2003).
[19] Antisymmetrization follows from the second-quantized operators used in the DMRG.
[20] J. Gauss, in *Encyclopedia of Computational Chemistry*, edited by P. R. Schleyer, W. L. Jorgensen, H. F. Schaefer, III, P. R. Schreiner, and W. Thiel (Wiley, New York, 1998), p. 615.
[21] T. Crawford and H. Schaefer, Rev. Comp. Chem. **14**, 33 (2000).
[22] M. Kállay and P. R. Surján, J. Chem. Phys. **113**, 1359 (2000).
[23] M. Kállay and P. R. Surján, J. Chem. Phys. **115**, 2945 (2001).
[24] S. Hirata and R. J. Bartlett, Chem. Phys. Lett. **321**, 216 (2000).
[25] J. Olsen, J. Chem. Phys. **113**, 7140 (2000).
[26] S. Hirata, J. Chem. Phys. **107**, 9887 (2003).
[27] M. Kállay, P. G. Szalay, and P. R. Surján, J. Chem. Phys. **117**, 980 (2002).
[28] N. Oliphant and L. Adamowicz, J. Chem. Phys. **96**, 3739 (1992).
[29] J. Paldus and X. Li, Adv. Chem. Phys. **110**, 1 (1999).
[30] R. D. Amos, A. Bernhardsson, A. Berning *et al.*, MOLPRO, a package of *ab initio* programs designed by H.-J. Werner and P. J. Knowles, release 2002.1 (2002).
[31] The small matrix sizes associated with higher symmetry groups led to memory fragmentation and loss of performance when running our code for extended periods. This is a feature of the dynamic memory allocation routine and not of our algorithm.
[32] J. Stanton, J. Gauss, J. Watts, W. J. Lauderdale, and R. J. Bartlett, Int. J. Quantum Chem. **S26**, 879 (1992).
[33] H. Lischka, R. Shepard, I. Shavitt *et al.*, Columbus, an *ab initio* electronic structure program, release 5.9 (2001).
[34] P. Pulay, Chem. Phys. Lett. **73**, 393 (1980).

RIGHTSLINK